Interaction of 300-GeV Protons with Uranium*

S. K. Chang† and Nathan Sugarman

Enrico Fermi Institute, The University of Chicago

5630 South Ellis Avenue, Chicago, Illinois 60637

Submitted to

Physical Review C, "Communications"

Interaction of 300-GeV Protons with Uranium*

S. K. Chang† and Nathan Sugarman

Enrico Fermi Institute, The University of Chicago
5630 South Ellis Avenue, Chicago, Illinois 60637

(Received   )

The cross sections and thick-target recoil properties of thirty nuclides produced in the interaction of 300-GeV protons with a ^{238}U target have been measured. The cross sections were determined relative to the monitor reaction $^{27}Al(p,3pn)^{24}Na$, whose cross section was assumed to be constant above 10 GeV. The average cross section of all products is found to be $\sim 10\%$ lower at 300 GeV than at 11.5 GeV. The recoil ranges of observed nuclides are $\sim 8\%$ shorter than at lower proton energy and F/B values are closer to unity. A preliminary study of the effect of secondary particles is presented.

[Nuclear reactions $^{238}U(p,F$ and Spallation), E = 300 GeV; measured σ and thick-target recoil properties of thirty product nuclides.]

I. INTRODUCTION

The interaction of 300-GeV protons with complex nuclei is currently being studied. Spallation cross sections for V,[1] Co,[1] and Ag[2] targets have recently been reported. These represent targets of low to medium mass. On the assumption that the cross section of the monitor reaction $^{27}Al(p,3pn)^{24}Na$ remains unchanged above 10 GeV, the spallation yields from these targets were found to be essentially independent of the incident proton energy. In this report, we present the cross sections and recoil properties of various product nuclides with mass number between 45 and 177 from U irradiated with 300-GeV protons. The results are compared with those obtained at lower proton energies.

II. EXPERIMENTAL PROCEDURE AND RESULTS

Four irradiations were performed in the external 300-GeV proton beam at the Neutrino Area of the National Accelerator Laboratory. The target assemblies are shown in Fig. 1. In two irradiations, the target consisted of a ~ 50 mg/cm^2 U foil sandwiched between two ~ 7 mg/cm^2 Al foils and wrapped by another Al foil (Fig. 1a). In two other experiments, in order to study the effect of secondary particles, three U foils, each surrounded by Al foils, were used (Fig. 1b). The length of irradiations varied from 10 hr to 24 hr. After

the irradiation, a circular area of 2.4 cm^2 was punched out.
The Al monitor foils were counted on β-proportional counters
for the ^{24}Na activities. The target and catcher foils were
dissolved in the presence of carriers. Standard chemical pro-
cedures[3] were followed for separation and yield determination.
Activity measurements on the chemically separated samples were
made with proportional counters for β emitters, a 2-mm NaI
crystal for X rays, a Ge(Li) X-ray detector and Ge(Li) γ-ray
detectors. The efficiencies of the detectors were calibrated
with sources of known energy and disintegration rate. The decay
properties and the measured radiations of the observed nuclides
are listed in Table I. The decay curves were analyzed by the
Cumming CLSQ[4] computer code. The radioactivity of the target was
corrected for counter efficiency, branching ratio, chemical
yield, and recoil loss. The cross sections are determined
relative to that of the ^{27}Al(p,3pn)^{24}Na reaction whose value
is assumed to be 8.6 mb at 300 GeV.[1,2] The variation of incident
beam intensity during the irradiation was taken into account in
the calculation of saturation factors.

The results of the cross-section measurements at 300
GeV are listed in Column 6 of Table II, with the number of
determinations in parentheses. The values given are those
obtained with a $\sim$ 50 mg/cm^2 U target foil assembly (Fig. 1a)
uncorrected for secondary particle effects in the Al monitor

or the U target. The precision of the measurements, as determined from separate experiments or from counting statistics when only one experiment was performed, is the order of 5%. The (I) or (C) adjacent to the nuclides of Column 1 refers to independent or cumulative production, respectively. The previously reported cross sections at lower energies (3-28 GeV) are also given in Table II. In order to minimize the uncertainty in the decay scheme and detector efficiency calibration in the comparison of cross-section results at 300 GeV with those at lower energy, cross sections of several nuclides were also studied at 11.5 GeV.[5] These irradiations were performed at the Zero Gradient Synchrotron of the Argonne National Laboratory. The same chemical procedures and counting equipment were used and the data were analyzed in the same way as in the 300-GeV experiments.

The thick target recoil properties measured at 300 GeV are given in Table III along with previously reported results at lower proton energies. F and B are the fractions of the total activity of the specific nuclide in the forward and backward catcher foils, respectively. W is the surface density of the uranium target in mg/cm^2 U. The 2W(F+B) values have been corrected for edge and scattering effects.[6]

III. DISCUSSION

From Table II it can be seen that the cross sections for all product nuclides from U measured at 300 GeV are generally somewhat smaller than those observed at 11.5 GeV. The mean cross section ratio, $\sigma_{300}/\sigma_{11.5}$, for all measured products is 0.91 ± 0.13, compared with 0.96 ± 0.04 for V,[1] 1.02 ± 0.09 for Co[1] and 0.91 ± 0.07 for Ag.[2]   Thus, even for U the proton interaction with the nucleus leads to excited nuclei whose average deposition energy does not change significantly between 11.5 GeV and 300 GeV.

A more detailed examination of the $\sigma_{300}/\sigma_{11.5}$ ratio indicates a difference between products in the A < 70 mass region and those for 70 < A < 140. The average cross section ratio for products of A < 70 is 1.03 ± 0.14 whereas that for products of 70 < A < 140 is 0.83 ± 0.13. It would appear that the cross sections for nuclides in the binary fission mass region[7] at 300 GeV decreases by about 17% from those at 11.5 GeV while the cross sections for the products in the lighter mass region does not change. Further studies on products of the A < 40 mass region should be most informative.

The recoil properties, 2W(F+B) and F/B, of the measured product nuclides (Table III) are also changed somewhat from those at 11.5 GeV. The 2W(F+B) values are smaller at 300 GeV than at 11.5 GeV, the mean ratio $2W(F+B)_{300}/2W(F+B)_{11.5}$ being

0.93 ± 0.05, indicating a slightly lower mass for the average
excited nucleus at the higher energy. The F/B values are also
smaller at 300 GeV, implying that the incident proton imparts
less forward momentum to the excited nucleus. Beg and Porile[8]
studied the recoil properties of Sr and Ba nuclides as a
function of incident proton energy. They found that the F/B
values of the neutron-rich nuclides stay constant with
increasing proton energy, whereas those of neutron-deficient
nuclides go through a maximum at $\sim$ 3 GeV and then decrease
slowly with increasing energy. The values reported here for
300 GeV are a continuation of this trend.

A preliminary study of the effect of target thickness
on the cross section and recoil properties measured for thick
U target foils was made at 300 GeV. The purpose of this experi-
ment was the comparison of the effect of secondary particles
at 300 GeV with that at 11.5 GeV and 28 GeV on the production
of ^{24}Na in the Al monitor foils and the production and recoil
properties of neutron-deficient (^{103}Pd, ^{105}Ag, ^{106}Ag$\underline{m}$) and
neutron-excess (^{111}Ag) products from U in the target foil. The
results from two target assemblies, a $\sim$ 50 mg/cm^2 U target
(single target, Fig. 1a) and a 230 mg/cm^2 U target (multiple
target assembly, Fig. 1b), are given in Table IV. The first
row of Table IV gives the results for the $\sim$ 50 mg/cm^2 U target;
the second row, the results for the combined thick U target,

230 mg/cm^2 U; the third, fourth and fifth rows, the results for the individual U targets of the combined target.

A comparison of the results of the $\sim$ 50 mg/cm^2 U target with those of the 230 mg/cm^2 U target shows that the results for neutron-deficient products are not affected by target thickness whereas those for [111]Ag are to about the same extent observed at 11.5 GeV[9,10] and 28 GeV.[11] The "upstream" build-up of secondary production of [111]Ag is evident from the increase in the cross section along the path of the combined target. That there is also an effect of target thickness on the production of [24]Na from Al is evident from the ratio M_F/M_B (Fig. 1a) of 1.02 for the $\sim$ 50 mg/cm^2 U target and the ratio M_2/M_1 (Fig. 1b) of 1.15 for the combined target. It is estimated from these results that the secondary production of [24]Na in the Al monitor foil and of the neutron excess products in U is $\sim$ 11% for a 100 mg/cm^2 U target, essentially the same as that reported at lower energies.[10,11]

IV. CONCLUSION

The cross sections and thick-target recoil properties of thirty nuclides produced in the interaction of 300 GeV protons with uranium have been measured. The recoil range values [2W(F+B)] of all products are slightly lower than those observed at lower energy and the F/B ratios are closer to unity. The cross sections of product nuclides in the mass region 40 < A < 70 are about the same as at 11.5 GeV, while those in the mass region 70 < A < 140 are ~ 15% lower. Although pion production in proton-proton interaction is known to increase with proton energy,[12] the evidence from these experiments and others[1,2] points to a relatively constant deposition energy spectrum, implying noninteraction of the extra pions with the nucleus. The production of nuclides by secondary particles is about the same as observed at lower energy.[10,11] Radiochemical studies in the mass regions A < 40 and 140 < A < 238, along with charge dispersion measurements, are necessary for a more complete comparison of the interaction of 300 GeV protons with U compared to that at lower energy.

REFERENCES

1. S. Katcoff, S. B. Kaufman, E. P. Steinberg, M. W. Weisfield, and B. D. Wilkins, Phys. Rev. Lett. $\underline{30}$, 1221 (1973).

2. G. English, Y. W. Yu, and N. T. Porile, Phys. Rev. Lett. $\underline{31}$, 244 (1973).

3. "Collected Radiochemical Procedures", Los Alamos Scientific Laboratory Report LA-1721, 3rd Ed., 1967.

4. J. B. Cumming, National Academy of Sciences Report No. NAS-NS-3107, 1962 (unpublished) p. 25.

5. S. K. Chang and Nathan Sugarman (unpublished).

6. J. A. Panontin and Nathan Sugarman, J. Inorg. Nucl. Chem. $\underline{25}$, 1321 (1963).

7. Y. Y. Chu, E. M. Franz, G. Friedlander, and P. J. Karol, Phys. Rev. $\underline{C4}$, 2202 (1971).

8. K. Beg and N. T. Porile, Phys. Rev. $\underline{C3}$, 1631 (1971).

9. A. F. Stehney and E. P. Steinberg, Nucl Instr. and Meth. $\underline{59}$, 102 (1968).

10. Y. W. Yu and N. T. Porile, Phys. Rev. $\underline{C7}$, 1597 (1973).

11. Y. Y. Chu, E. M. Franz, and G. Friedlander, Nucl. Phys. $\underline{134B}$, 428 (1972).

12. F. T. Dao, D. Gordon, J. Lach, E. Malamud, T. Meyer, R. Porter, and W. Slater, Phys. Rev. Lett. $\underline{29}$, 1627 (1972).

Table I. Decay properties of the observed radionuclides[a]

Nuclide	Mode of Decay	$t_{1/2}$	Radiation Measured	Branching Ratio
^{45}Ca	β^-	165 d	β^-	1.0
^{47}Ca	β^-	4.5 d	1.31 MeV γ	0.74
^{59}Fe	β^-	45.6 d	1.095 MeV γ	0.56
^{56}Co	EC, β^+	77.3 d	0.847 MeV γ	1.00
^{57}Co	EC	270 d	0.122 MeV γ	0.87
^{58}Co	EC, β^+	71.3 d	0.810 MeV γ	0.99
^{60}Co	β^-	5.26 y	1.173 MeV γ	1.00
^{64}Cu	β^-, β^+, EC	12.8 hr	0.511 MeV γ	0.38
^{67}Cu	β^-	61.7 hr	0.185 MeV γ	0.41
^{82}Sr	EC	25 d	0.511 MeV γ[b]	1.92
^{83}Sr	EC, β^+	33 hr	0.511 MeV γ	0.32
^{85}Sr	EC	64 d	0.514 MeV γ	1.00
^{89}Sr	β^-	52.7 d	β^-	1.00
^{91}Sr	β^-	9.7 hr	0.651 MeV γ	0.12
^{93}Mo$^{\underline{m}}$	IT	6.9 hr	0.685 MeV γ	1.00
^{99}Mo	β^-	66.7 hr	β^-	1.00
^{100}Pd	EC	3.7 d	0.084 MeV γ	0.49

Table I. (Continued)

Nuclide	Mode of Decay	$t_{1/2}$	Radiation Measured	Branching Ratio
^{103}Pd	EC	17 d	X-ray	0.78
^{109}Pd	β^-	13.5 hr	0.088 MeV γ	0.042
^{111}Pd$\underline{^m}$	β^-, IT	5.5 hr	0.175 MeV γ	0.31
^{112}Pd	β^-	21 hr	0.621 MeV γ	0.41
^{105}Ag	EC	40 d	0.280 MeV γ	0.32
^{106}Ag$\underline{^m}$	EC	8.4 d	0.512 MeV γ	0.86
^{110}Ag$\underline{^m}$	β^-, IT	253 d	0.658 MeV γ	0.96
^{111}Ag	β^-	7.5 d	β^-	1.00
^{128}Ba	EC	2.4 d	0.511 MeV γ[b]	1.10
^{131}Ba	EC	12.0 d	0.122 MeV γ	0.28
^{133}Ba$\underline{^m}$	IT	39 hr	0.278 MeV γ	0.17
^{135}Ba$\underline{^m}$	IT	28.7 hr	0.268 MeV γ	0.16
^{140}Ba	β^-	12.8 d	0.537 MeV γ	0.20
^{177}Ta	EC	56.6 hr	X-ray	0.94

a   Data taken from "Table of Isotopes", C. M. Lederer, J. M.

Hollander and I. Perlman (Wiley, New York, 1967), 6th Ed. and

current "Nuclear Data Sheets", Edited by Nuclear Data Group,

D. J. Horen, Director (Academic Press, New York).

b   Daughter activity.

Table II. Formation cross sections of products from
multi-GeV proton bombardment of uranium (in mb)

Nuclide	3 GeV	6 GeV	11.5 GeV[a]	28 GeV	300 GeV[b]	$\sigma_{300}/\sigma_{11.5}$
^{45}Ca (C)	3.7[c]				3.28 (2)	0.89[d]
^{47}Ca (C)	1.2[c]				1.59 (2)	1.33[d]
^{59}Fe (C)			5.0[j]		4.8 (3)	0.96
^{56}Co (C)			0.31[j]		0.32 (2)	1.03
^{57}Co (I)			1.45[j]		1.54 (3)	1.06
^{58}Co (I)			3.8[j]		4.0 (2)	1.05
^{60}Co (I)			5.0[j]		5.4 (3)	1.08
^{64}Cu (C)			2.9[j]		2.5 (2)	0.86
^{67}Cu (C)	4.7[e]	3.7[h]	2.9[j]		2.8 (3)	0.97
^{83}Sr (C)	4.1[f]	7.1[f]	5.8[f]	3.32[l]	3.16 (1)	0.54
^{85}Sr (C)					6.26 (1)	
^{89}Sr (C)					24.3 (1)	
^{91}Sr (C)	14.2[f]	14.7[f]	14.3[f]	17.1[l]	13.6 (1)	0.80
^{93}Mo$^{\underline{m}}$ (C)		2.2[h]	2.3[j]		2.20 (2)	0.97
^{99}Mo (C)		25[h]	23.5[j]		23.4 (4)	1.00
^{100}Pd (C)	0.88[g]		0.90[k]	1.31[l]	0.85 (3)	0.94
^{103}Pd (C)	3.6[g]		5.1[k]	4.1[g]	3.21 (2)	0.78

Table II. (Continued)

Nuclide	3 GeV	6 GeV	11.5 GeV[a]	28 GeV	300 GeV[b]	$\sigma_{300}/\sigma_{11.5}$
^{109}Pd (C)	21.4[g]	19.1[i]	18.3[j]	18[l]	17.2 (3)	0.94
^{111}Pd$^{\underline{m}}$ (I)	5.5[g]	2.2[i]	4.04[j]	3.9[g]	3.2 (1)	0.79
^{112}Pd (C)	16.9[g]		15.0[j]	14.3[g]	14.3 (1)	0.95
^{105}Ag (C)			2.01[j]		1.78 (3)	0.89
^{106}Ag$^{\underline{m}}$ (I)			1.80[j]		1.52 (3)	0.84
^{110}Ag$^{\underline{m}}$ (I)			3.27[j]		2.47 (3)	0.76
^{111}Ag (C)		21.5[h]	24.3[k]		17.6 (4)	0.72
^{128}Ba (C)	5.1[f]	6.6[f]	6.5[f]	6.0[l]	4.9 (1)	0.75
^{131}Ba (C)	8.2[f]	9.4[f]	8.8[f]		6.2 (1)	0.70
^{133}Ba$^{\underline{m}}$ (I)					8.1 (1)	
^{135}Ba$^{\underline{m}}$ (I)					1.23 (1)	
^{140}Ba (C)	7.4[f]	7.6[f]	7.8[f]	10.0[l]	7.4 (1)	0.95
^{177}Ta (C)			2.85[j]		2.96 (2)	1.04

a. Average precision ~ 4%.

b. Average precision ~ 5%.

c. G. Friedlander and L. Yaffe, Phys. Rev. 117, 578 (1960).

d. σ_{300}/σ_3.

e. S. Kaufman, Phys. Rev. 129, 1866 (1963).

f. Reference 8.

Table II. (Continued)

g. N. T. Porile, Phys. Rev. 148, 1235 (1966).

h. J. M. Alexander, C. Baltzinger and M. F. Gazdik, Phys. Rev. 129, 1826 (1963).

i. R. H. Shudde, University of California Laboratory Report UCRL 3419 (1956), unpublished.

j. Reference 5.

k. J. A. Panontin and N. T. Porile, J. Inorg. Nucl. Chem. 32, 1775 (1970).

ℓ. Reference 11. Results corrected for secondary effects.

Table III. Thick target recoil properties of product nuclides
from multi-GeV proton bombardment of uranium

| Nuclide | 3 GeV | | 6 GeV | | 11.5 GeV[a,c] | | 300 GeV[b,c] | | $\dfrac{2W(F+B)_{300}}{2W(F+B)_{11.5}}$ |
	$2W(F+B)$, mg/cm^2 U	F/B	$2W(F+B)$, mg/cm^2 U	F/B	$2W(F+B)$, mg/cm^2 U	F/B	$2W(F+B)$, mg/cm^2 U	F/B	
^{45}Ca							9.51	1.02	
^{47}Ca							8.43	1.06	
^{64}Cu			8.0	1.25[e]	8.05	1.08[f]	7.05	1.01	0.88
^{67}Cu			9.9	1.13[e]	9.76	1.11[f]	8.90	1.08	0.91
^{83}Sr	8.04	1.32[d]	6.35	1.18[d]	6.12	1.18[d]	5.27	1.09	0.86
^{85}Sr							4.89	1.08	
^{89}Sr							8.63	1.03	
^{91}Sr	10.22	1.03[d]	10.23	1.08[d]	10.09	1.09[d]	9.53	1.05	0.94
^{93}Mo$^{\underline{m}}$					5.83	1.12[g]	5.84	1.07	1.00
^{99}Mo			9.3	1.15[e]	9.51	1.06[g]	9.24	1.05	0.97
^{100}Pd					4.68	1.11[g]	4.00	1.03	0.85
^{103}Pd					5.48	1.13[g]	4.68	1.08	0.85

Table III. (Continued)

Nuclide	3 GeV 2W(F+B), mg/cm^2 U	F/B	6 GeV 2W(F+B), mg/cm^2 U	F/B	11.5 GeV[a,c] 2W(F+B), mg/cm^2 U	F/B	300 GeV[b,c] 2W(F+B), mg/cm^2 U	F/B	$\dfrac{2W(F+B)_{300}}{2W(F+B)_{11.5}}$
^{109}Pd					8.83	1.09[g]	8.62	1.06	0.98
^{111}Pd$\underline{^{m}}$					9.39	1.10[g]	8.70	1.11	0.93
^{112}Pd			8.1	1.17[e]	9.47	1.08[g]	8.68	1.11	0.92
^{105}Ag					4.66	1.24[g]	4.06	1.15	0.87
^{106}Ag$\underline{^{m}}$					5.70	1.21[g]	5.46	1.09	0.96
^{110}Ag$\underline{^{m}}$					7.98	1.12[g]	7.66	1.11	0.96
^{111}Ag			8.1	1.17[e]	8.72	1.12[g]	7.98	1.11	0.92
^{128}Ba	4.15	1.80[d]	3.34	1.50[d]	2.99	1.25[d]	2.89	1.21	0.97
^{131}Ba	4.46	1.66[d]	3.92	1.41[d]	3.58	1.27[d]	3.38	1.25	0.94
^{133}Ba$\underline{^{m}}$							4.75	1.36	
^{135}Ba$\underline{^{m}}$							6.85	1.23	
^{140}Ba	7.27	1.08[d]	8.06	1.07[d]	7.95	1.04[d]	7.49	1.05	0.94
^{177}Ta					0.96	2.11[g]	0.91	1.85	0.95

Table III. (Continued)

a. Average precision $\sim$ 4%.

b. Average precision $\sim$ 6%.

c. Values corrected for edge and scattering effects (Reference 6).

d. Reference 8.

e. J. M. Alexander, C. Baltzinger, and M. F. Gazdik, Phys. Rev. 129, 1826 (1963).

f. S. K. Chang and Nathan Sugarman, Phys. Rev. C8, 775 (1973).

g. Reference 5.

Table IV. Effect of target thickness on the cross section and recoil properties at 300 GeV

Target thickness, mg/cm^2 U	^{103}Pd			^{105}Ag			$^{106}Ag\underline{m}$			^{111}Ag		
	σ, mb	2W(F+B), mg/cm^2 U	F/B	σ, mb	2W(F+B), mg/cm^2 U	F/B	σ, mb	2W(F+B), mg/cm^2 U	F/B	σ, mb	2W(F+B), mg/cm^2 U	F/B
~ 50	3.21	4.68	1.08	1.78	4.06	1.15	1.52	5.46	1.09	17.6	7.98	1.11
230	3.28			1.79	3.93	1.13	1.43			19.5	7.93	1.34
0 - 48.5	3.38	4.59	1.07	1.82	3.89	1.12	1.50	5.33	1.08	18.3	7.83	1.17
48.5-177.5	3.26	4.77	1.08	1.78			1.40			19.6		
177.5-230	3.26			1.81	3.89	1.14	1.46			20.3	8.06	1.17

Fig. 1. Target assemblies for cross-section and recoil
measurements. (a) Single U target, $\sim$ 50 mg/cm^2.
(b) Multiple uranium target. A, Al wrapper foil;
M, Al monitor; F and B, forward and backward catcher
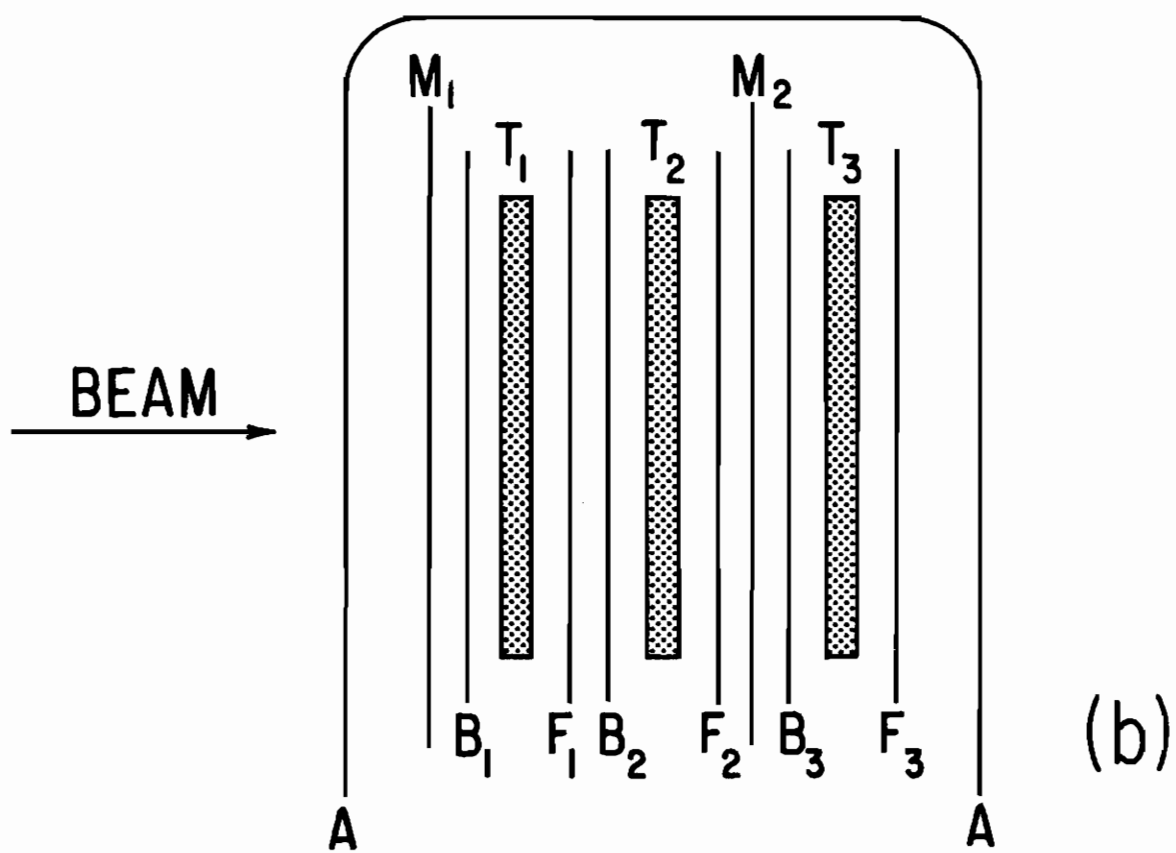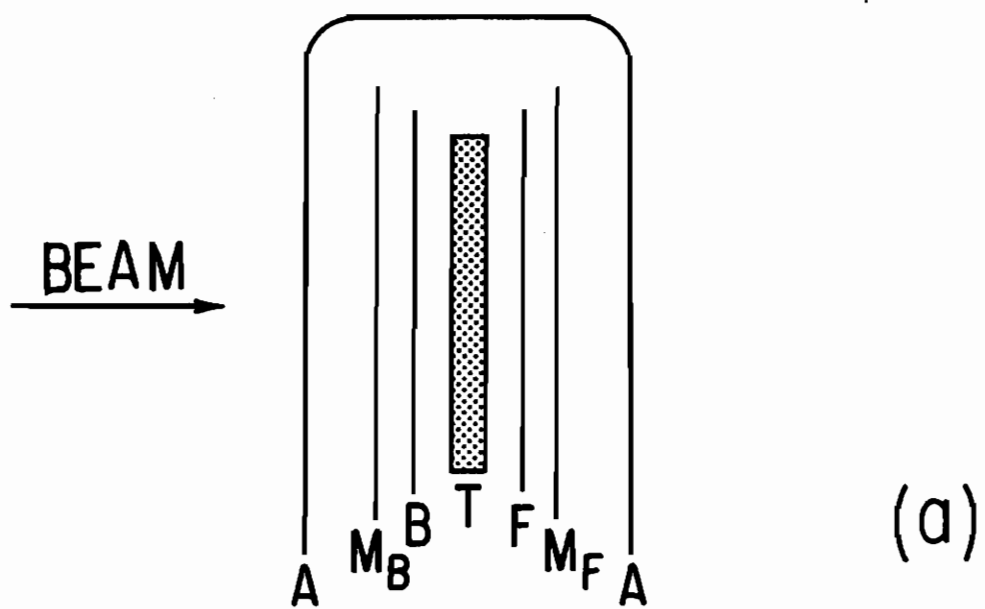foils, respectively; T, U target foil.

BEAM →

A   M$_B$ B T F M$_F$ A

(a)

BEAM →

M$_1$ T$_1$ T$_2$ M$_2$ T$_3$

A   B$_1$ F$_1$ B$_2$ F$_2$ B$_3$ F$_3$ A

(b)

Fig. 1